IFP35 family proteins promote neuroinflammation and multiple sclerosis

Xizhong Jing[a], Yongjie Yao[a], Danning Wu[b], Hao Hong[a], Xu Feng[b], Na Xu[b], Yingfang Liu[a,c,1], and Huanhuan Liang[b,1]

[a]School of Medicine, Sun Yat-sen University, Shenzhen 518107, China; [b]School of Pharmaceutical Sciences (Shenzhen), Sun Yat-sen University, Shenzhen 518107, China; and [c]Guangdong Provincial Key Laboratory of Colorectal and Pelvic Floor Diseases, The Sixth Affiliated Hospital, Sun Yat-sen University, Guangzhou 510275, China

Edited by Lawrence Steinman, Stanford University School of Medicine, Stanford, CA, and approved June 11, 2021 (received for review February 15, 2021)

Excessive activation of T cells and microglia represents a hallmark of the pathogenesis of human multiple sclerosis (MS). However, the regulatory molecules overactivating these immune cells remain to be identified. Previously, we reported that extracellular IFP35 family proteins, including IFP35 and NMI, activated macrophages as proinflammatory molecules in the periphery. Here, we investigated their functions in the process of neuroinflammation both in the central nervous system (CNS) and the periphery. Our analysis of clinical transcriptomic data showed that expression of IFP35 family proteins was up-regulated in patients with MS. Additional in vitro studies demonstrated that IFP35 and NMI were released by multiple cells. IFP35 and NMI subsequently triggered nuclear factor kappa B–dependent activation of microglia via the TLR4 pathway. Importantly, we showed that both IFP35 and NMI activated dendritic cells and promoted naïve T cell differentiation into Th1 and Th17 cells. *Nmi*$^{-/-}$, *Ifp35*$^{-/-}$, or administration of neutralizing antibodies against IFP35 alleviated the immune cells' infiltration and demyelination in the CNS, thus reducing the severity of experimental autoimmune encephalomyelitis. Together, our findings reveal a hitherto unknown mechanism by which IFP35 family proteins facilitate overactivation of both T cells and microglia and propose avenues to study the pathogenesis of MS.

neuroinflammation | multiple sclerosis | microglia activation | T cell activation | DAMP

Multiple sclerosis (MS) is a chronic inflammatory demyelinating disease within the central nervous systems (CNS). Pathological characteristics of MS include inflammatory cell infiltration, myelin sheath destruction, focal demyelination, axon damage, and neurodegeneration (1). MS is the major cause of nontraumatic disability in young adults, imposing significant burden on MS patients and their families (2). Despite intensive experimental and clinical research on the pathogenesis of MS, the etiology and precise molecular mechanism underlying the initiation and progression of the disease remains obscure.

The dysregulated immune system is believed to be predominantly responsible for the exacerbation of MS (3). Multiple immune cells, including T cells (4), as well as microglia (5) and resident macrophages, are thought to collaboratively cause damage to the myelin sheaths, oligodendrocytes, axons, and neurons. Autoreactive T cells primarily initiate an inflammatory response against myelin autoantigens following enter the CNS (6). Th1 and Th17 cells produce IFN-γ, TNFα, GM-CSF, and IL-17, which promote the activation of microglia and macrophages. In turn, activated microglia are the major source of many neurotoxic factors, including nitric oxide (NO), reactive oxygen species, cyclooxygenase-2 (COX-2), TNFα, proteases, and glutamate (7), thus facilitating excessive neuroinflammation responses and resulting in pathogenic encephalomyelitis. In addition, cytokines and chemokines derived from activated microglia and T cells facilitate the recruitment of peripheral immune cells into the CNS (8). In contrast, immune responses mediated by Th2 (9) and Treg (10) cells are generally associated with inflammation reduction and beneficial effects on clinical symptoms of MS patients. To study the molecular mechanisms underlying MS, the experimental autoimmune encephalomyelitis (EAE) model is most commonly used, since it exhibits clinical and immunopathological characteristics similar to those found in MS patients (11).

Although several disease-modifying treatments (DMTs), like IFNβ agents, are clinically used to alleviate MS symptoms (12), MS remains incurable as its precise etiology and pathogenesis remains under-researched. Therefore, elucidating the network of factors required for activation of T cells and microglia is critical for finding suitable therapeutic targets. Recent evidence showed that inflammatory responses are exacerbated by a group of endogenous molecules known as proinflammatory damage-associated molecular patterns (DAMPs) (13). Following cellular stress or tissue injury, DAMPs are released from cells into the extracellular space by activated immune cells and damaged cells. These released DAMPs are recognized by specific pattern recognition receptors (PRRs) (14), (e.g., TLRs, NLRs, and RIG-I), resulting in wide-ranging activation of immune responses in both the CNS and periphery (15, 16). Since breakdown cell debris in MS lesions are an abundant resource of DAMPs (17, 18), DAMPs may act as inadvertent contributors to inflammatory processes that persist beyond the normal immune response, causing injuries of neurological tissues during the development of MS.

IFP35 (interferon-induced protein 35) family proteins including NMI (N-myc and STAT-interacting protein) and IFP35 were originally identified as interferon-inducible proteins functioning both in transcriptional regulation and anti-viral responses (19–21). Previously, we found that the IFP35 members are released by lipopolysaccharide (LPS)–activated macrophages and act as DAMPs

Significance

Multiple sclerosis (MS) is a complex neuroinflammatory disorder that constitutes the major cause of nontraumatic disability in young adults. However, the underlying mechanism of this disease remains obscure. Here, we identified NMI and IFP35 as factors critical in the progress of MS and experimental autoimmune encephalomyelitis, as their dysregulation activates both microglia in the central nervous system and T cells in the periphery. This study expands our understanding of the pathogenesis of MS and aims to provide potential diagnostic and therapeutic targets.

Author contributions: Y.L. and H.L. designed research; X.J., Y.Y., D.W., H.H., X.F., and N.X. performed research; X.J., Y.L., and H.L. analyzed data; and X.J., Y.L., and H.L. wrote the paper.

The authors declare no competing interest.

This article is a PNAS Direct Submission.

[1]To whom correspondence may be addressed. Email: liuyingf5@mail.sysu.edu.cn or lianghh26@mail.sysu.edu.cn.

This article contains supporting information online at https://www.pnas.org/lookup/suppl/doi:10.1073/pnas.2102642118/-/DCSupplemental.

Published August 6, 2021.

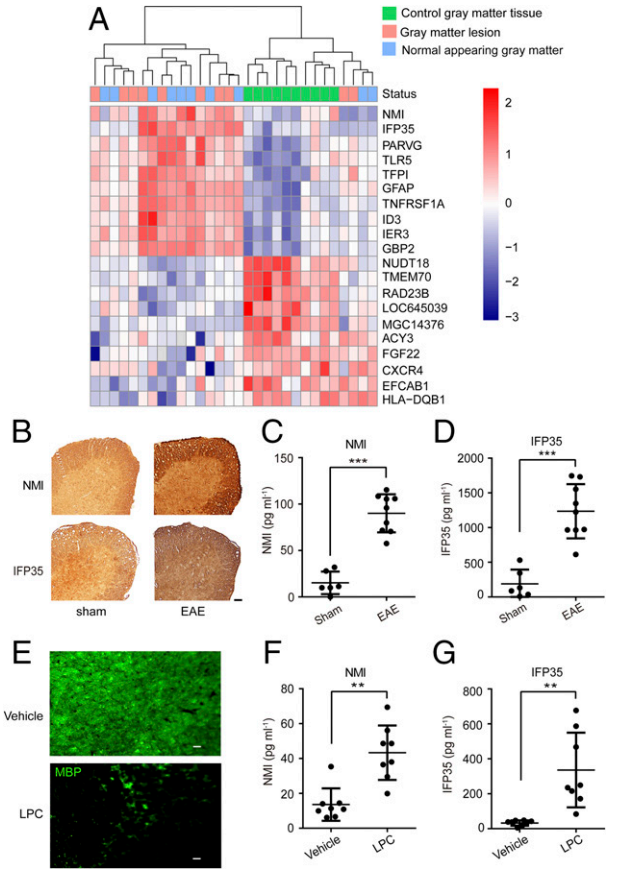

Fig. 1. The expression and release of NMI and IFP35 in MS patients and mice models. (*A*) Heatmap of genes expressed differentially in the gray matter of MS patients. Gene expression is hierarchically clustered and presented as row-wise Z scores of normalized expression level. Dendrogram of differentially expressed genes and samples clustered are shown on the top. (*B*) Immunohistochemistry staining of NMI and IFP35 expression in the spinal cord of sham (left panel) or EAE (right panel) mice 20 d after immunization. (Scale bar: 50 μm.) (*C* and *D*) NMI or IFP35 released in the sera of sham mice or mice 20 d after EAE immunization and detected by ELISA. $n = 6$ to 9 mice in each group. (*E*) Immunofluorescent staining of MBP expressed in the cerebellar slice after vehicle or LPC (0.5 mg · mL^{-1}) treated for 48 h in vitro. (Scale bar: 20 μm.) (*F* and *G*) NMI or IFP35 released in the vehicle- or LPC-incubated culture were detected by ELISA. $n = 8$. Data are presented as mean ± SD. Significance was tested by two-tailed unpaired Student's *t* test, $^{**}P < 0.01$. $^{***}P < 0.001$.

to promote and amplify host inflammatory responses in sepsis (22). A number of recent reports showed that IFP35 family proteins are also involved in multiple inflammatory diseases, including hepatitis B virus–related acute-on-chronic liver failure (23), chronic obstructive pulmonary disease (24), and lupus nephritis (25). One recent clinical study demonstrated that the expression levels of IFP35 are correlated with the progression and clinical outcome of neuroinflammation in MS patients (26). However, the precise mechanisms functionally linking IFP35 family proteins and MS remain obscure. Here, we analyzed the function of IFP35 family proteins in microglia activation and Th polarization using both in vitro and EAE model.

Results

Increased Expression of IFP35 and NMI in MS and Demyelinating Models. To investigate whether IFP35 family proteins are involved in MS, we first analyzed the transcription levels of *Nmi* and *Ifp35* in gray matter lesions and normal-appearing gray matter (NAGM) areas of MS patients. Data from gray matter tissues of healthy donors were used as controls. The transcriptomic datasets of MS patients and healthy donors were downloaded from Gene Expression Omnibus (accession code GSE135511). The heatmap of this analysis showed that the expression of *Nmi* and *Ifp35* in most of the gray matter and NAGM areas of MS patients was higher than that in healthy controls (Fig.1*A*).

We then examined whether IFP35 and NMI are expressed in neuronal cells and immune cells of the CNS. We first measured the expression of IFP35 and NMI in the spinal cords of C57BL/6 mice using immunofluorescent staining assay. Spinal cord tissues were fixed and immune-stained with antibodies against NeuN, GFAP, and CD11b to detect neuron cells, astrocytes, and microglia, respectively. As shown in *SI Appendix*, Fig. S1 *A* and *C*, we found that IFP35 family proteins localized inside of these cells in the spinal cords. We also used immortalized cells, including SH-SY5Y (neuron cells), C8-D1A (astrocytes), and BV2 (microglia) cells to confirm by immuno-staining experiments that IFP35 and NMI were broadly expressed in these CNS cells (*SI Appendix*, Fig. S1 *B* and *D*).

To verify the increased expression of NMI and IFP35 in MS, we employed two demyelinating models, namely EAE model and lysophosphatidylcholine (LPC)–induced model. In the EAE model, mice were immunized using $MOG_{35–55}$ emulsified with complete Freund's adjuvant (CFA). Immunohistochemical staining analysis showed that the expression of IFP35 and NMI increased in

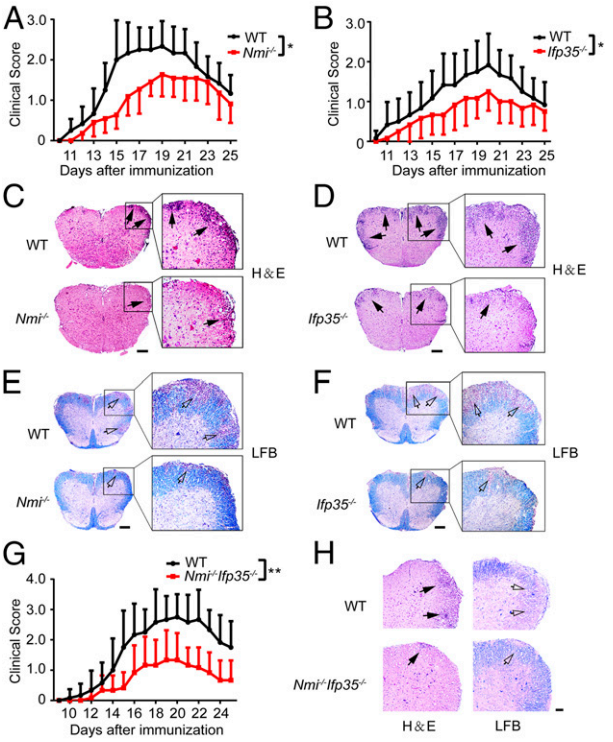

Fig. 2. NMI and IFP35 deficiency alleviated EAE symptoms and inflammation. (*A* and *B*) The mean clinical scores of EAE development in WT, *Nmi*$^{-/-}$, and *Ifp35*$^{-/-}$, mice ($n = 12$). (*C* and *D*) H&E staining of the spinal cord of the C57BL/6 WT, *Nmi*$^{-/-}$, and *Ifp35*$^{-/-}$ mice 20 d post model establishment. Solid black arrows indicate infiltrating areas. (Scale bar: 200 μm.) (*E* and *F*) LFB–PAS staining of the spinal cord of the EAE mice 20 d post model establishment. Hollow arrows indicate demyelinating areas. (Scale bar: 200 μm.) (*G*) Mean clinical scores of EAE development in WT and *Nmi*$^{-/-}$*Ifp35*$^{-/-}$ mice ($n = 12$). (*H*) H&E- and LFB-staining of the spinal cord of the WT and *Nmi*$^{-/-}$*Ifp35*$^{-/-}$ mice showing inflammatory infiltration and demyelination, respectively. (Scale bar: 100 μm.) $n = 12$ mice per group. Data are presented as mean ± SD. Significance was tested by two-way ANOVA test. $^{*}P < 0.05$ and $^{**}P < 0.01$.

the spinal cords of EAE mice compared with those in sham mice (primed with CFA alone) (Fig. 1*B*). Furthermore, we measured the expression levels of NMI and IFP35 proteins in the sera of EAE mice. The average concentrations of NMI and IFP35 in the sera of sham mice were 15.20 ± 12.18 pg · mL^{-1} and 189.90 ± 205.03 pg · mL^{-1}, respectively. However, the average concentrations of these two proteins in the sera of EAE mice significantly increased to 90.07 ± 20.52 pg · mL^{-1} and 1,235.03 ± 391.07 pg · mL^{-1}, respectively (Fig. 1 *C* and *D*). LPC is an endogenous lysophospholipid known to nonspecifically disrupt myelin lipids and induce demyelination (27). As shown in Fig. 1*E*, the expression of myelin basic protein (MBP), a major constituent of the myelin sheath, was significantly lower in the cerebellar slices post–LPC treatment (0.5 mg · mL^{-1} for 48 h) compared to that treated with vehicle as control. The concentrations of NMI and IFP35 in the culture of vehicle were 13.61 ± 9.28 pg · mL^{-1} and 32.46 ± 15.43 pg · mL^{-1}, respectively. In comparison, we measured concentrations of NMI and IFP35 of approximately 43.35 ± 15.65 pg · mL^{-1} and 335.85 ± 213.60 pg · mL^{-1}, respectively, post–treatment with LPC (Fig. 1 *F* and *G*). Together, these results clearly demonstrated that the expression of IFP35 family proteins was elevated in both MS and demyelinating models.

IFP35 and NMI Deficiency Alleviated EAE Development. To investigate whether IFP35 family proteins are involved in the development of demyelinating diseases, we studied the effects of *Nmi*$^{-/-}$ or *Ifp35*$^{-/-}$ on the progression of EAE. Mice immunized with $MOG_{35–55}$ and CFA were monitored for their clinical signs of neuroinflammation (e.g., limp tail, paralyzed tail, hind limbs and forelimbs paralyzed, and moribund) for 25 d. A clinical score ranging from 0 (no symptoms) to 5 (moribund) was recorded for each mouse daily. Our analysis showed that all wide type (WT), *Nmi*$^{-/-}$ and *Ifp35*$^{-/-}$ mice developed EAE symptoms approximately 10 d post-immunization. However, compared with the

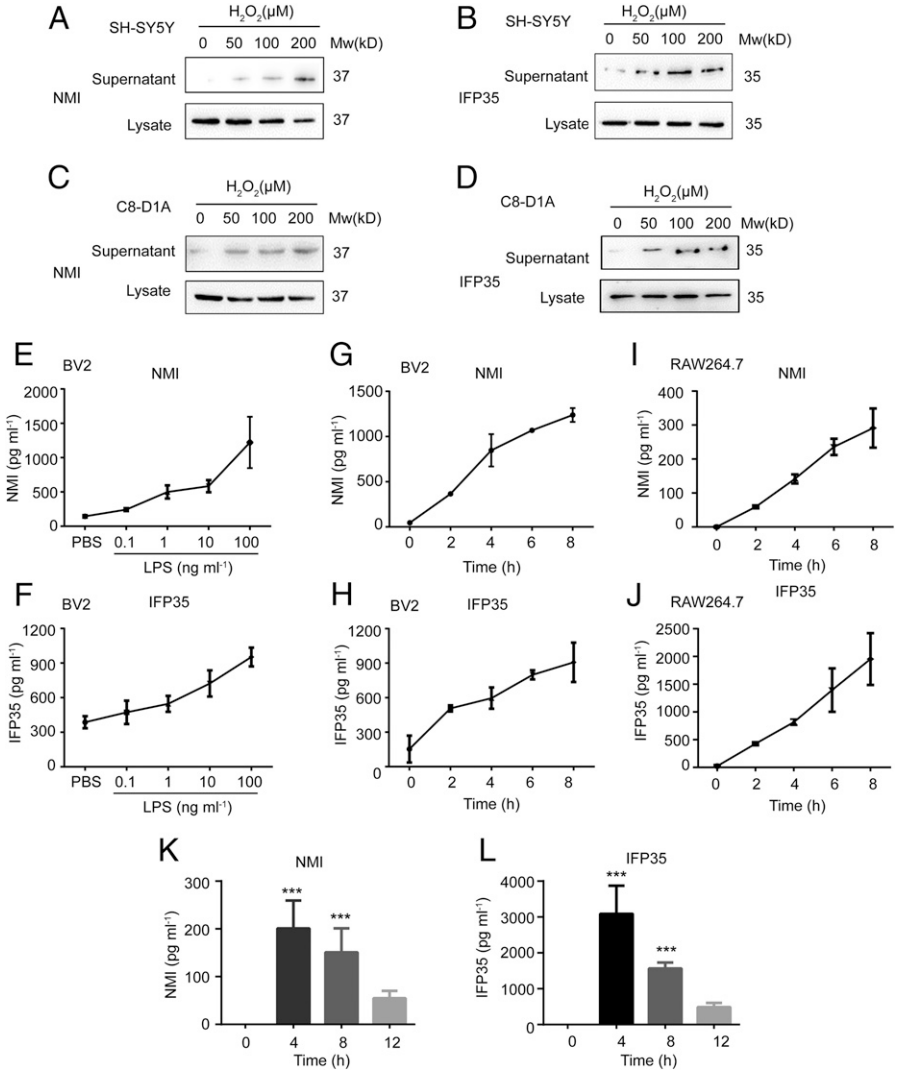

Fig. 3. NMI and IFP35 released in the CNS and periphery. (*A* and *B*) Released NMI and IFP35 in the supernatants of SH-SY5Y cells 24 h post H_2O_2 (0, 50, 100, and 200 μM) treatment and detected by Western blotting. (*C* and *D*) NMI and IFP35 released in the supernatants of C8-D1A cells treated with different concentrations of H_2O_2 and detected by Western blotting. Cell lysate was detected as control in *A–D*. (*E* and *F*) NMI and IFP35 released in the culture medium of BV2 cells stimulated by different concentration of LPS (0, 0.1, 1, 10, and 100 ng · mL^{-1}) for 8 h. (*G* and *H*) NMI and IFP35 released in the culture medium of BV2 cells stimulated by 100 ng · mL^{-1} of LPS for 0, 2, 4, 6, and 8 h. (*I* and *J*) NMI and IFP35 released in the culture medium of RAW264.7 cells stimulated with bacillus Calmette–Guérin (10 μg · mL^{-1}) for 0, 2, 4, 6, and 8 h. (*K* and *L*) Mice were intraperitoneally injected with bacillus Calmette–Guérin (10 mg · kg^{-1}). The serum concentrations of NMI and IFP35 in mice were determined by ELISA. $n = 4$ mice for each group. Data are presented as the mean ± SD. Significance was tested by one-way ANOVA. ***$P < 0.001$.

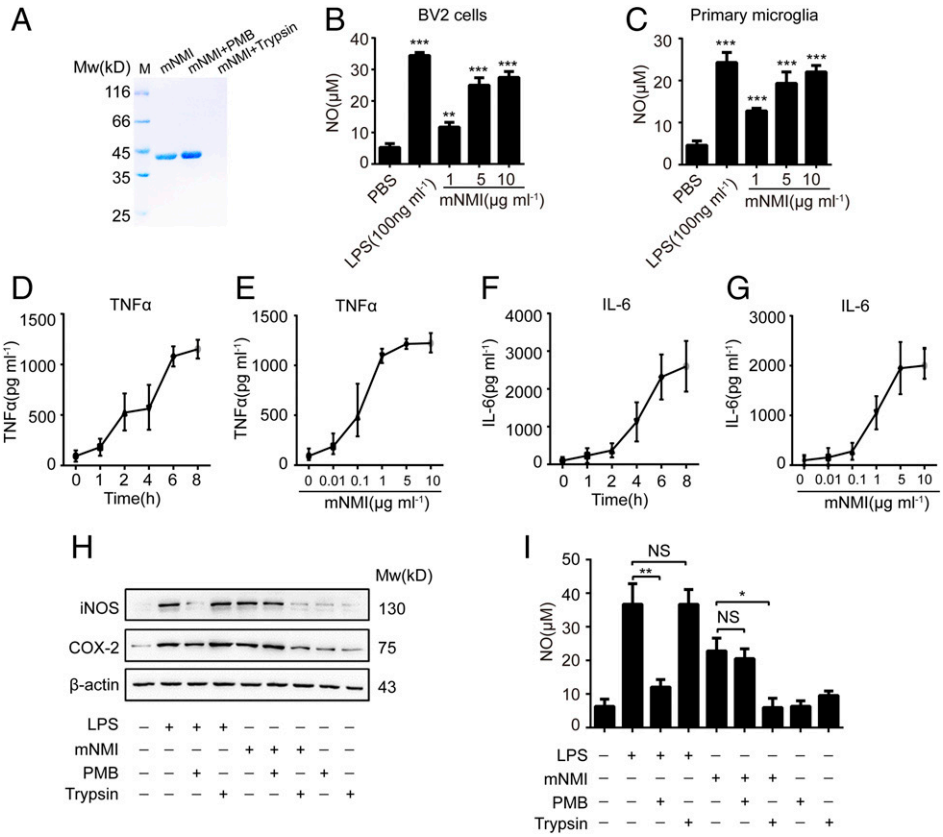

Fig. 4. Recombinant NMI induces the activation of microglia. (*A*) SDS-PAGE analysis and Coomassie blue staining of the recombinant mNMI protein used in microglia activation. (*B* and *C*) NO released by BV2 cells or primary microglia incubated with LPS (100 ng · mL^{-1}) or different concentrations of mNMI (1, 5, and 10 μg · mL^{-1}) for 24 h. (*D*–*G*) TNFα and IL-6 production in BV2 cells stimulated with mNMI (5 μg · mL^{-1}) for up to 8 h or increasing concentrations of recombinant mNMI. The concentrations of TNFα and IL-6 in supernatant were determined by ELISA. (*H*) The expression of iNOS and COX-2 in BV2 cells treated with mNMI (5 μg · mL^{-1}) or LPS (100 ng · mL^{-1}) for 24 h with (+) or without (–) pretreatment of polymysin (PMB, 25 μg · mL^{-1}), trypsin (5 μg · mL^{-1}, 37 °C overnight), and detected using Western blotting. (*I*) The production of NO in BV2 cells was detected using Griess reagent. Data are presented as mean ± SD from three biological replicates. Significance was tested by two-tailed unpaired Student's *t* test. *$P < 0.05$, **$P < 0.01$, and ***$P < 0.001$.

WT mice, the *Nmi*$^{-/-}$ and *Ifp35*$^{-/-}$ mice showed milder symptoms and lower clinical scores at the peak stage from day 16 to day 21 (Fig. 2 *A* and *B*). Next, we collected the spinal cord tissues at the peak stage and examined the inflammation and demyelination using hematoxylin-eosin (H&E) and luxol fast blue (LFB) staining. The H&E staining showed that the *Nmi*$^{-/-}$ and *Ifp35*$^{-/-}$ mice exhibited a lower degree of inflammatory cells infiltration when compared to WT mice (Fig. 2 *C* and *D*). Similarly, LFB–periodic acid-Schiff (PAS) staining showed that the demyelination areas of the spinal cord were reduced in *Nmi*$^{-/-}$ and *Ifp35*$^{-/-}$ mice (Fig. 2 *E* and *F*). This result is in agreement with the milder symptoms and lower clinical scores of these mice.

In addition to *Nmi*$^{-/-}$ and *Ifp35*$^{-/-}$ mice, we generated *Nmi* and *Ifp35* double-knockout mice (*Nmi*$^{-/-}$*Ifp35*$^{-/-}$) by crossing *Nmi*$^{-/-}$ and *Ifp35*$^{-/-}$ mice and subjected *Nmi*$^{-/-}$*Ifp35*$^{-/-}$mice to EAE. Our results showed that the clinical scores of *Nmi*$^{-/-}$*Ifp35*$^{-/-}$ mice were significantly lower compared to the scores of WT mice (Fig. 2*G*). In agreement with this result, we found that inflammatory cell infiltration and demyelination were lower in the spinal cord of *Nmi*$^{-/-}$*Ifp35*$^{-/-}$ mice compared to control mice (Fig. 2*H*). Importantly, the effects of *Nmi*$^{-/-}$*Ifp35*$^{-/-}$ in reducing EAE symptoms were better than that in *Nmi*$^{-/-}$ or *Ifp35*$^{-/-}$, suggesting that these two genes act in a synergistic manner. Together, these data suggested that both IFP35 family proteins contributed to the pathogenesis of EAE.

NMI and IFP35 Were Released by Cells Both in the CNS and Periphery. Since NMI and IFP35 levels were elevated in the CNS of MS patients and sera of EAE mice, we examined whether they were released by damaged cells in CNS. We stimulated SH-SY5Y or C8-D1A cells with hydrogen peroxide (H_2O_2) to induce oxidative damage. The extracellular NMI and IFP35 proteins in the cultures were detected thereafter using Western blotting. As shown in Fig. 3 *A*–*D*, both NMI and IFP35 were released in the cultures of the SH-SY5Y and C8-D1A cells in the presence of 50 to 200 μM H_2O_2.

To test whether NMI and IFP35 released from activated immune cells in the CNS, we stimulated BV2 cells with LPS and measured the secreted IFP35 family proteins using enzyme-linked immunosorbent assay (ELISA). Upon induction with LPS (0 to 100 pg · mL^{-1}) for 8 h, the extracellular NMI gradually increased from 144.13 ± 17.17 pg · mL^{-1} to 1,221.31 ± 373.99 pg · mL^{-1}, and IFP35 increased from 386.58 ± 52.56 pg · mL^{-1} to 952.65 ± 81.19 pg · mL^{-1} in a dose-dependent manner (Fig. 3 *E* and *F*). The released NMI also increased from 45.17 ± 14.37 pg · mL^{-1} to 1,238.00 ± 76.24 pg · mL^{-1} and IFP35 from 152.88 ± 117.04 pg · mL^{-1} to 906.97 ± 170.42 pg · mL^{-1} post–LPS (100 pg · mL^{-1}) stimulation for 0 to 8 h in a time-dependent manner (Fig. 3 *G* and *H*).

To examine whether NMI and IFP35 are also released by the peripheral immune cells during EAE progression, we stimulated RAW264.7 macrophage cells with *Bacillus* Calmette–Guérin (bacillus Calmette–Guérin), one component of the EAE induction reagent and potent activator of macrophage. After

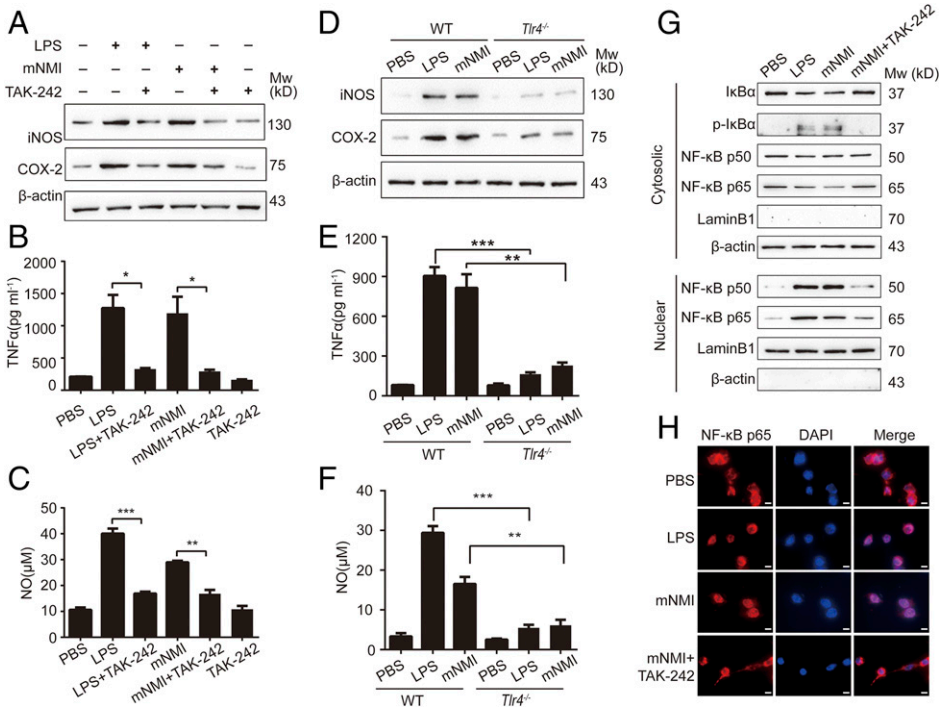

Fig. 5. Proinflammatory effects of NMI is mediated via toll-like receptor 4 (TLR4) and NF-κB pathway. (*A*) The expression of iNOS and COX-2 in BV2 cells treated with mNMI (5 μg · mL^{-1}) or LPS (100 ng · mL^{-1}) for 24 h with (+) or without (–) pretreatment of TAK-242 (100 nM, 2 h) and detected using Western blotting. (*B* and *C*) TNFα (*B*) and NO (*C*) in the supernatants of BV2 cells were detected by ELISA and Griess reagent, respectively. (*D*) The expression of iNOS and COX-2 in primary microglia from WT or *Tlr4*$^{-/-}$ mice treated with mNMI (5 μg · mL^{-1}) or LPS (100 ng · mL^{-1}) for 24 h. (*E* and *F*) TNFα and NO in the supernatant of primary WT or *Tlr4*$^{-/-}$ microglia detected as shown in panel *B* and *C*. (*G*) BV2 cells were treated with LPS (100 ng · mL^{-1}), mNMI (5 μg · mL^{-1}), or mNMI (5 μg · mL^{-1}) together with TAK-242 (100 nM) for 1 h. IκB, p-IκB, and NF-κB (p50 and p65) in the cytoplasm and NF-κB (p50 and p65) protein in nucleus extracts from BV2 cells were assessed by Western blotting. β-actin in the cytoplasm and LaminB1 in the nucleus were used as control. (*H*) The localization of NF-κB p65 was examined using immunofluorescent staining. The cells were counterstained with 4,6-diamino-2-phenyl indole (DAPI) to show nuclei. (Scale bar: 10 μm.) Data are presented as mean ± SD from three biological replicates. Significance was tested by two-tailed unpaired Student's *t* test. **P* < 0.05, ***P* < 0.01, and ****P* < 0.001.

incubation of RAW264.7 cells with bacillus Calmette–Guérin–containing growth media (10 μg · nmL^{-1}) for 8 h, NMI and IFP35 levels were measured in the cell culture. As shown in Fig. 3 *I* and *J*, levels of NMI and IFP35 released by RAW264.7 cells increased from 0 pg · mL^{-1} to 291.22 ± 57.61 pg · mL^{-1}, and IFP35 released from 24.54 ± 25.95 pg · mL^{-1} to 1,953.02 ± 467.04 pg · mL^{-1}, respectively.

To verify the in vitro results under more physiological conditions, we measured the release of NMI and IFP35 in vivo. To this end, we injected mice intraperitoneally with 100 μg · kg^{-1} bacillus Calmette–Guérin. As shown in Fig. 3 *K* and *L*, the levels of NMI and IFP35 in the sera of healthy control mice were almost undetectable. In contrast, 4 h post–bacillus Calmette–Guérin injection, NMI and IFP35 in the sera reached the peaks at 200.97 ± 58.39 pg · mL^{-1} and 3,089.46 ± 781.68 pg · mL^{-1}, respectively.

Given that NMI and IFP35 are released after cell damage or immune activation, we hypothesized that the up-regulation and release of IFP35 and NMI are mediated by inflammatory factors from activated immune cells. To test this hypothesis, we stimulated BV2 and RAW264.7 cells with IFN-γ (10 ng · mL^{-1}) and IL-2 (2 μM), two Th1 effector molecules, for up to 24 h. The results showed that both messenger RNA (mRNA) levels and protein expression of IFP35 and NMI increased with time in both cell lines (*SI Appendix*, Fig. S5). Together, these results clearly demonstrated that during injury and inflammation, NMI and IFP35 were up-regulated and released by multiple cells both in the CNS and periphery.

NMI-Activated Nuclear Factor Kappa B Pathway in Microglia through Toll-Like Receptor 4. To study the immunoregulation function of NMI in CNS, we stimulated microglia using recombinant mouse NMI (mNMI) protein (Fig. 4*A*). The full-length mNMI protein was expressed and purified as described in the previous report (22). To eliminate possible endotoxin contamination during protein purification, we pretreated mNMI protein with polymyxin B (PMB, 25 μg · mL^{-1}), a cationic polypeptide antibiotic that binds to the anionic lipid A portion of LPS and neutralizes its endotoxin capacity. Production of NO through inducible NO synthase (iNOS) is a hallmark of microglia activation. As shown in Fig. 4 *B* and *C*, both BV2 cells and primary microglia generated NO in a dose-dependent manner after incubating the cells with mNMI protein for 24 h. The activity of mNMI at 5 μg · mL^{-1} was comparable to that of 100 ng · mL^{-1} LPS. In addition, TNFα and IL-6 secreted by BV2 cells also increased with both dose- and time-dependent manner upon mNMI induction (Fig. 4 *D*–*G*). In addition, the expression of iNOS and COX-2 in BV2 cells considerably increased after LPS or mNMI treatment. The activity of mNMI was abolished after trypsin digestion (5 μg · mL^{-1}, 37 °C overnight). In contrast, trypsin treatment failed to affect LPS activity, while PMB treatment greatly decreased the activity of LPS (Fig. 4*H*). Similar to the expression of iNOS and COX-2, the production of NO by mNMI-stimulated BV2 cells was affected by trypsin treatment (Fig. 4*I*).

We attempted to obtain a full-length IFP35 protein; however, we failed presumably because the recombinant IFP35 protein was produced inside inclusion bodies. We then generated an N-terminally truncated form of human IFP35 protein, termed

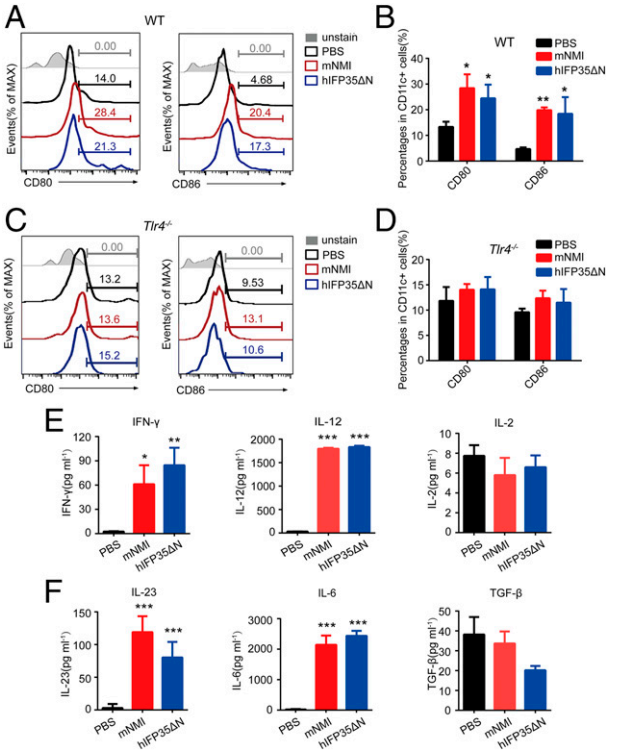

Fig. 6. Recombinant NMI and IFP35 proteins induce the DC activation in vitro. (*A–D*) Flow-cytometric analysis of $CD80^+$ and $CD86^+$ in $CD11c^+$ BMDCs, which were isolated from bone marrow of WT (*A* and *B*) or $Tlr4^{-/-}$ (*C* and *D*) mice and incubated with recombinant mNMI or hIFP35ΔN protein for 48 h. (*E* and *F*) The Th1-promoting cytokines IFN-γ, IL-12, IL-2, and Th17 promoting cytokines IL-23, IL-6, and TGF-β in the culture supernatants of BMDCs in *A* were detected by ELISA. $n = 4$. Data are shown as the mean ± SD. Significance was tested by one-way ANOVA. $*P < 0.05$, $**P < 0.01$, and $***P < 0.001$.

hIFP35ΔN, which included residues 31 through 289 of hIFP35 with a GST tag (*SI Appendix*, Fig. S2*A*). We treated BV2 cells with hIFP35ΔN and GST protein as control. Due to the high sequence conservation between hIFP35ΔN and mouse IFP35 (identity > 70%), hIFP35ΔN induced the release of TNFα and IL-6 in BV2 cells in a time-dependent manner (*SI Appendix*, Fig. S2 *B–E*). Taken together, these results suggested that the extracellular NMI and IFP35 function as a potent stimulus inducing microglia activation as well as production of proinflammatory factors.

We previously reported that NMI induces nuclear factor kappa B (NF-κB) activation through TLR4 signaling pathway in macrophage (22). Thus, we hypothesized that NMI also activates microglia through the TLR4 pathway. To verify this hypothesis, we suppressed the TLR4 signaling pathway of microglia using TAK-242, a known TLR4 inhibitor. As shown in Fig. 5*A* and *SI Appendix*, Fig. S3*A*, the activity of recombinant mNMI inducing the expression of iNOS and COX-2 was greatly reduced in TAK-242–pretreated BV2 cells. Similarly, TAK-242 also abrogated the ability of mNMI inducing the release TNFα and NO by BV2 cells (Fig. 5 *B* and *C*). In agreement with these results, the capability of NMI to elicit the expression and release of these proinflammatory factors was also abolished in $Tlr4^{-/-}$ primary microglia (Fig. 5 *D–F* and *SI Appendix*, Fig. S3*B*).

We next examined the effects of NMI on NF-κB activation in microglia, which is intensively involved in the pathogenic progression of EAE and MS (28, 29). After incubating BV2 cells in culture with mNMI protein (5 μg · mL^{-1}), we found that IκB, the inhibitory protein of NF-κB, was phosphorylated and degraded in the cytoplasm. The subunits of NF-κB, p50 and p65, decreased in the cytoplasm and increased in the nuclear (Fig. 5*G* and *SI Appendix*, Fig. S3 *C* and *D*). The translocation of p65 from cytoplasm to nuclear was also observed using immunofluorescent staining (Fig. 5*H*). The translocation of NF-κB p65 subunit triggered by NMI was abolished by TAK-242 (Fig. 5 *G* and *H* and *SI Appendix*, Fig. S3 *C* and *D*). Together, these results suggested that extracellular IFP35 family proteins elicit the NF-κB–dependent proinflammatory responses of microglia through the TLR4 signaling pathway.

Both NMI and IFP35 Promoted the Activation of Dendritic Cells and Proinflammatory Th Cells. To obtain a more comprehensive immune response profile, we further assessed whether extracellular IFP35 family proteins are required in the activation of dendritic cells (DCs) and T cells, which are important in both initiation and progression of MS (30). The DCs used in this experiment were acquired from murine bone marrow cells and induced with GM-CSF (20 ng · mL^{-1}) and IL-4 (5 ng · mL^{-1}) for 5 d as previously described (31). The bone marrow–derived DCs (BMDCs) were incubated for 48 h with either recombinant mNMI or hIFP35ΔN proteins (5 μg · mL^{-1}). Next, we assessed the expression of CD80 and CD86, the two biomarkers of mature DCs using flow cytometry. The proportions of $CD80^+$ $CD11c^+$ and $CD86^+$ $CD11c^+$ cells obtained from WT mice increased from 13.30 ± 2.55 and 4.67 ± 0.67% to 26.43 ± 5.49% and 19.13 ± 4.22%, respectively, after the BMDCs were incubated with recombinant proteins (Fig. 6 *A* and *B*). In contrast, neither recombinant mNMI nor hIFP35ΔN protein induced an increase of $CD80^+$ $CD11c^+$ and $CD86^+$ $CD11c^+$cells in BMDCs obtained from $Tlr4^{-/-}$ mice (Fig. 6 *C* and *D*). These results suggested that IFP35 family proteins mediated the maturation of DCs also through activating the TLR4 pathway.

Since cytokines released by mature DCs act as crucial regulators for the differentiation of T cells (32), we next assessed the levels of cytokines in the culture of BMDCs. Following treatment of BMDCs with either mNMI or hIFP35ΔN protein, we found that both Th1 regulatory cytokines (IFN-γ and IL-12) as well as Th17 regulatory cytokines (IL-23 and IL-6) significantly increased in the culture media (Fig. 6 *E* and *F*). In contrast, we found that the levels of other regulatory cytokines, IL-2 and TGF-β, changed insignificantly. Together, these results suggested that extracellular IFP35 family proteins promote DC maturation, cytokine production, and thus may influence the differentiation of Th cells.

We then isolated and purified $CD4^+$ T cells from the draining lymph nodes (LNs) of mice. The $CD4^+$ T cells were cocultured with or without IFP35 family proteins stimulated BMDCs for 5 d. The proportions of IFN-γ^+ and $IL17A^+$ T cells were measured by flow cytometry. As shown in Fig. 7 *A* and *B*, the proportions of IFN-γ^+ and $IL17A^+$ $CD4^+$ T cells significantly increased from 1.09 ± 0.45% and 0.23 ± 0.11% to 3.05 ± 0.71% and 1.42 ± 0.60%, respectively, after coculturing with IFP35 family proteins stimulated BMDCs. In addition, the concentrations of IFN-γ and IL17A in the culture increased from 3.07 ± 3.56 pg · mL^{-1} and 9.05 ± 4.46 pg · mL^{-1} to 188.15 ± 52.26 pg · mL^{-1} and 134.13 ± 61.57 pg · mL^{-1}, respectively (Fig. 7*C*). These results suggested that IFP35 family proteins promote DCs maturation and proinflammatory T cells differentiation. We next verified these in vitro results in EAE model using WT and $Nmi^{-/-}Ifp35^{-/-}$ mice. The IFN-γ^+ $CD4^+$ T and $IL17A^+$ $CD4^+$ T cells in the LN and SP were measured 18 d post–EAE induction. Our results showed that the percentages of both IFN-γ^+ $CD4^+$ and $IL17A^+$ $CD4^+$ T cells in the peripheral lymphoid organs were significantly lower in $Nmi^{-/-}Ifp35^{-/-}$ mice compared to those in WT mice (Fig. 7 *D–F*). Together, our results demonstrated that IFP35 family proteins

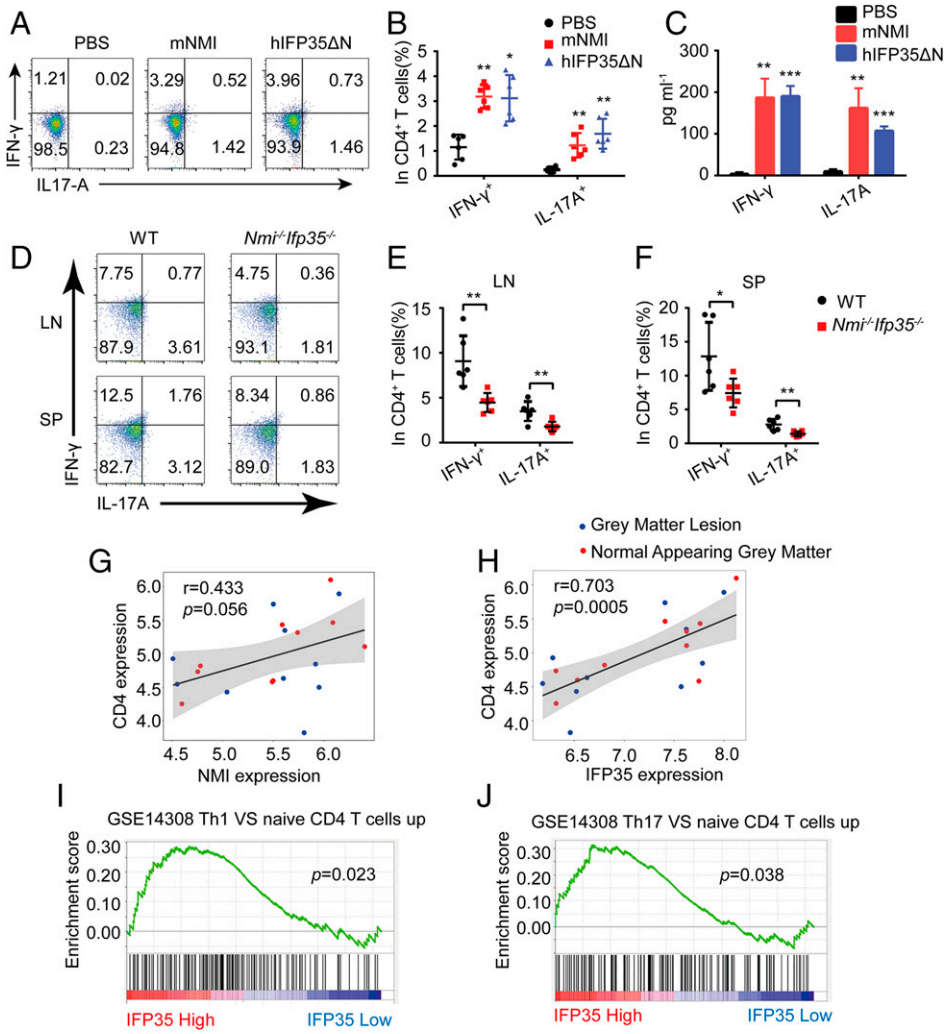

Fig. 7. IFP35 family proteins regulated Th1 and Th17 activation in vitro and in vivo. (*A* and *B*) Autologous CD4$^+$ T cells were isolated from SPs or LNs of WT mice and cocultured with or without mNMI- or hIFP35Δ*N*-stimulated BMDCs. After 5 d of incubation, the expression of Th1 (IFN-γ$^+$) and Th17 (IL-17A$^+$) cells in CD4$^+$ cells were analyzed using flow cytometry. (*C*) IFN-γ and IL-17A in the cocultured supernatants were detected by ELISA. $n = 6$. Data are shown as the mean ± SD. Significance was tested by one-way ANOVA. $^*P < 0.05$, $^{**}P < 0.01$, and $^{***}P < 0.001$. (*D–F*) Flow-cytometric analysis of IFN-γ$^+$ and IL-17A$^+$ cells in CD4$^+$ cells in the draining LN and SP of WT and *Nmi*$^{-/-}$*Ifp35*$^{-/-}$ mice 18 d post–EAE induction. $n = 6$. Data are shown as the mean ± SD. Significance was tested by two-tailed unpaired Student's *t* test. $^*P < 0.05$ and $^{**}P < 0.01$. (*G* and *H*) The linear correlation between the relative expression of CD4 and NMI and IFP35 in gray matter tissues of patients with MS. Pearson r and *P* values are shown and tested with Pearson test. (*I* and *J*) GSEA of gene sets up-regulated in Th1 or Th17 cells polarization compared to naïve CD4 T cells performed using the transcriptome of gray matter tissues of patients with MS.

promote proinflammatory T cells differentiation both in vitro and in vivo.

Next, we examined whether NMI and IFP35 affect the effector Th1 and Th17 cytokines production. To this end, we immunized WT, *Nmi*$^{-/-}$, and *Ifp35*$^{-/-}$ mice with $MOG_{35–55}$ and CFA and harvested the LN and spleen (SP) 12 d later. Subsequently, we cultured single-cell suspensions of LN and SP with different concentrations of $MOG_{35–55}$ for 72 h before harvesting. Th1 cytokines (TNF-α, IFN-γ) and Th17 cytokines (GM-CSF, IL-17A) in the culture were measured by ELISA. As shown in *SI Appendix*, Fig. S4 *A* and *B*, cells from *Nmi*$^{-/-}$ or *Ifp35*$^{-/-}$ mice produced less TNF-α, IFN-γ, GM-CSF, and IL-17A in the presence of high dose of $MOG_{35–55}$. This result indicated that IFP35 family proteins are associated with proinflammatory Th response.

To assess how expression levels of IFP35 family proteins correlate with Th response, we studied the clinical MS transcriptomic data. The correlation between the expression level of CD4 and IFP35 family proteins was analyzed in gray matter lesions and NAGM of patients with MS. Our results showed a positive linear correlation between the expression level of CD4 and IFP35 family proteins (Fig. 7 *G* and *H*). In addition, the correlation between the expression of IFP35 and the enrichment of gene sets of Th1 and Th17 cell polarization (33) was evaluated using transcriptome gene set enrichment analysis (GSEA). Compared to that in naïve CD4$^+$ T cells, gene sets associated with Th1 and Th17 cells were enriched with high expression levels of IFP35 in the gray matter tissues of MS patients (Fig. 7 *I* and *J*). Taken together, these results suggested that NMI and IFP35 proteins are associated with the proinflammatory Th immune response both in EAE model and MS clinical course.

NMI- and IFP35-Deficiency T Cells Attenuated Passive EAE. To further verify the impacts of NMI and IFP35 on Th cell function during EAE pathogenesis, we employed a passive EAE model established as previously described (34). We isolated and purified CD4$^+$ T cells from SPs and LNs of WT and *Nmi*$^{-/-}$*Ifp35*$^{-/-}$ mice 12 d after EAE immunization and cultured them with $MOG_{35–55}$ for 4 d in vitro. The stimulated T cells were intravenously injected to

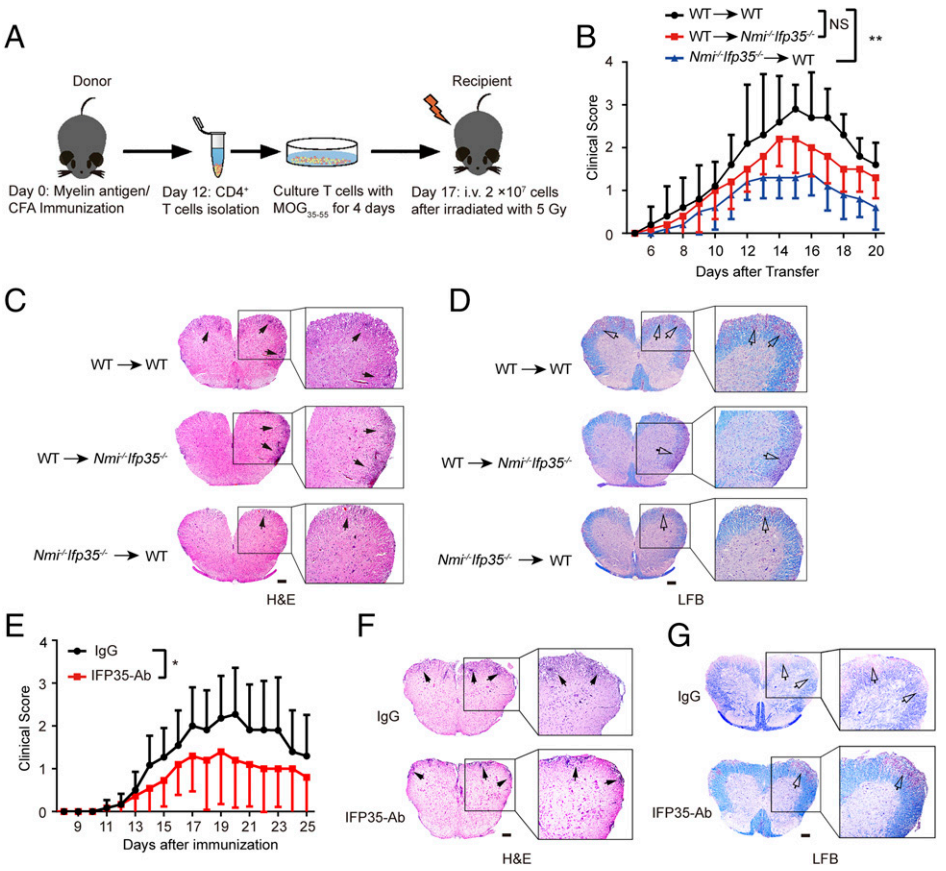

Fig. 8. NMI and IFP35 deficiency alleviated passive EAE symptoms and administration of IFP35 neutralizing antibody relieved active EAE. (*A*) Schematic representation of the passive EAE experiments. (*B*) Mean clinical scores after CD4$^+$ T cells from WT or *Nmi*$^{-/-}$*Ifp35*$^{-/-}$ mice transferred to the WT or *Nmi*$^{-/-}$*Ifp35*$^{-/-}$ recipient mice. n = 10. Data are shown as mean ± SD (*C* and *D*) Representative images of H&E (*C*) and LFB (*D*) staining of the spinal cord sections of passively transferred mice. (Scale bar: 200 μm.) (*E*) The mean clinical scores of EAE development in IFP35-neutralizing antibody or IgG-treated mice. n = 10. Data are shown as mean ± SD (*F* and *G*) Representative images of H&E- and LFB-staining of the spinal cord sections of the IFP35 neutralizing antibody or IgG-treated mice. (Scale bar: 200 μm.) Solid black arrows indicate infiltrating areas. Hollow arrows indicate demyelinating areas. Significance was tested by two-way ANOVA test. *P < 0.05 and **P < 0.01.

sublethally irradiated (5Gy) WT or *Nmi*$^{-/-}$*Ifp35*$^{-/-}$ recipient mice (2×10^7 cells for each mouse) (Fig. 8*A*). Compared with the CD4$^+$ T cells from WT mice, CD4$^+$ T cells from *Nmi*$^{-/-}$*Ifp35*$^{-/-}$ mice induced markedly milder passive EAE pathogenesis in WT recipients. In addition, when recipient mice were applied to CD4$^+$ T cells from WT mice, *Nmi*$^{-/-}$*Ifp35*$^{-/-}$ recipients developed slightly milder EAE pathogenesis compared to WT recipients (Fig. 8*B*). H&E- and LFB-staining results confirmed that T cells from *Nmi*$^{-/-}$*Ifp35*$^{-/-}$ mice induced attenuated inflammatory cell invasion and demyelination in WT recipient mice (Fig. 8 *C* and *D*). Together, these results confirmed that IFP35 family proteins play important roles in encephalitic Th immune response in EAE.

IFP35 Neutralizing Antibody Therapy Relieved EAE Symptoms. As IFP35-deficient mice showed alleviated EAE pathogenesis, we next assessed whether IFP35 monoclonal neutralizing antibody (IFP35-Ab) alleviates EAE symptoms in WT mice. The IFP35-Ab was developed using a universal hybridoma method (35) and evaluated using LPS-induced sepsis model. The IFP35-Ab was administered to mice by intravenous injection daily (5 mg · kg^{-1}) from initial to peak stages (days 12 to 22) after EAE immunization. Compared to the control group (isotype antibody IgG), IFP35-Ab treatment significantly ameliorated EAE clinical progression with lower clinical scores (Fig. 8*E*). H&E -and LFB-staining also showed that IFP35-Ab relieved inflammatory infiltration and demyelination symptoms (Fig. 8 *F* and *G*).

Discussion

In this study, we found that IFP35 and NMI are overexpressed in the CNS of MS patients and demyelinating models. Both factors are released by multiple cells including macrophages, neurons, astrocytes, and microglia upon inflammation or injury. The extracellular IFP35 family proteins activate microglia though the TLR4 pathway and promote the differentiation of T cells via DC activation. In addition, we showed that gene knock-out or administration of neutralizing antibody against IFP35 alleviated the symptoms of EAE mice.

First, we demonstrate that IFP35 and NMI were released to extracellular space as DAMPs in EAE- and LPC-induced inflammation or injury demyelinating models (Fig. 1). Previous reports demonstrated that DAMPs are either passively released from necrotic cells or actively secreted from activated immune cells (36, 37). Infiltrating and resident immune cells were reported gather in the MS lesions (38) and lead to various manners of cell damage and death, such as apoptosis, pyroptosis, necrosis/necroptosis, and ferroptosis in EAE/MS lesions (39–42). The expression levels of many DAMPs, including HMGB1, S100A/B, heat shock proteins, and IL-33 were reported increased in the active lesions, cerebrospinal fluid, and serum in EAE/MS (17, 43–46). Thus, we proposed that the release pathway of IFP35 and NMI in MS is similar with those of other DAMPs. This is in agreement with a previous study showing that IFP35 and NMI are released by stimulated macrophages in periphery in sepsis model (22).

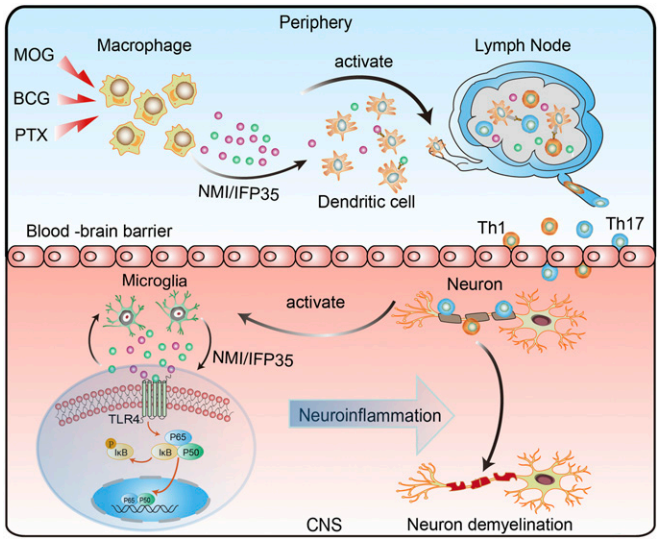

Fig. 9. Schematic illustration of the function of NMI and IFP35 in EAE pathogenesis. NMI and IFP35 are released by peripheral early activated macrophages post–EAE induction. The extracellular IFP35 family proteins promote the activation and differentiation of Th cells via activated DCs. Activated Th1 and Th17 cells infiltrate into CNS and trigger neuroinflammation. IFP35 family proteins released in the CNS further amplify activate microglia through TLR4/NF-κB pathway, thus driving the demyelination and progression of EAE.

In addition, we found that the extracellular IFP35 family proteins activated immune cells both in CNS and periphery. It is well accepted that DAMPs promote peripheral inflammation and inflammatory diseases (47), while the contribution of DAMPs to autoimmune attack in MS remain unclear. Our findings extend the knowledge of IFP35 family proteins and provide a mechanism for MS pathogenesis. In the periphery, the extracellular IFP35 and NMI activate macrophages and DCs and promote the expression of proinflammatory molecules, including NO, TNF-α, IFN-γ, IL-12, IL-23, and IL-6, which trigger innate immune activation and initiate subsequent specific autoimmune response by facilitating the differentiation of Th cells into proinflammatory Th1 and Th17 cells. This proinflammatory function of DAMPs has also been studied in DAMPs like HMGB1, IL-1α, IL-33, and S100 family proteins. Once dysregulated, these proteins play a key role in the development of acute or chronic inflammatory diseases (48). In addition to promoting Th differentiation through DCs activation, HMGB1 also directly induce naïve T cell differentiation into Th2 and Th17 cells by activating the TLR2, TLR4, and RAGE-NF-κB signal pathway (49). Whether IFP35 and NMI directly stimulate T cell activation needs further investigation. In the CNS, IFP35 and NMI activate microglia and resident macrophages through the TLR4 signaling pathway and promote more expression of proinflammatory cytokines. Furthermore, cytokines derived from activated Th1 cells, such as IFN-γ and IL-2, increase the expression of IFP35 family proteins in microglia and macrophage (*SI Appendix*, Fig. S5). This result is consistent with previous reports that the expression of IFP35 and NMI are up-regulated by interferons in HeLa cells, lymphocytes, fibroblasts, and tumor cells (19, 50, 51). Thus, extracellular IFP35 and NMI proteins mediate cross-talk between the immune cells in the periphery and the CNS and mediate positive feedback of the host immune response during EAE pathogenesis (Fig. 9).

While a small number of DMTs have been approved for the treatment of MS, DMT agents often failed to arrest the progression or relapse of MS due to considerable cost, drug resistance, and side effects. One recent clinical study showed significant increase of the IFP35 expression post–IFNβ treatment in MS patients (26), which may influence the long-term clinical outcome and drug efficacy. Targeting proinflammatory DAMPs themselves has been considered as a novel approach to normalize inflammation in MS, since it mainly restrains the pathogenic autoimmune response without compromising the host entire immune system (52). HMGB1 neutralization successfully ameliorated chronic or relapsing–remitting EAE by alleviating T cell activation and recruitment (53). Blockade of S100B also exhibited beneficial outcome in both in vitro and in vivo demyelinating models (54). Our results showed that administering of neutralizing antibodies against IFP35 ameliorated EAE clinical progression with ameliorative clinical symptoms, neuroinflammation, and demyelination (Fig. 8*E*). Thus, antibodies to relieve IFP35 and/or NMI would be a feasible approach for the treatment of MS.

Although our results showed that IFP35 and NMI function as proinflammatory factors in the EAE pathogenesis, several questions about them remain unclear. Firstly, IFP35 and NMI are particularly effective for activation of certain immune cells in our experimental system. For instance, IFP35 and NMI proteins are potent activators of innate immune cells, including microglia and macrophages. Our results showed that mNMI strongly trigger microglia activation via the TLR4-dependent pathway (Fig. 4). However, it only mildly activated T cells, since the difference between WT and NMI deficiency only sometimes achieved statistical significance (*SI Appendix*, Fig. S4). We attributed this to the fact that DAMPs can directly trigger microglia/macrophage activation upon binding to PRRs at the cell surface, while the activation of T cells is regulated by more delicate inflammatory regulation with antigen-presenting cells, costimulatory molecules, and a variety of cytokine participation (55). Further study about the precise regulatory mechanism of NMI and IFP35 in Th response is still needed. In addition, previous reports suggested that DAMPs are recognized by multiple PRRs at the surface or inside of immune cells (56). Our study showed that IFP35 family proteins activate microglia and DCs via the TLR4 pathway. However, other possible PRRs of NMI and IFP35 remain to be further explored. Furthermore, we found that IFP35 and NMI were broadly expressed in normal CNS tissues as well as in immortal cell lines. The functions of IFP35 family proteins in the CNS remain to be investigated in more detail.

In conclusion, our study identified an additional mechanism for the pathogenesis of MS, one of the most severe autoimmune neurodegenerative diseases that affects millions of people worldwide, and reveals potential diagnostic and therapeutic targets suitable to combat this disease.

Materials and Methods

Materials. Antibodies and regents used were included in *SI Appendix*.

Cell Stimulation. For cell stimulation experiments, mouse BV2 cells, primary microglia, SH-SY5Y, C8-D1A, RAW264.7, and BMDC cells were seeded in 6-well plates at a density of 2×10^6 cells per well and grew overnight. Then the cells were stimulated with varying concentrations of LPS, bacillus Calmette–Guérin, H_2O_2, and purified recombinant proteins mNMI and hIFP35ΔN for different time periods as indicated in the figures and figure legends.

Induction and Evaluation of EAE. C57BL/6 WT, *Nmi*$^{-/-}$, *Ifp35*$^{-/-}$, and *Nmi*$^{-/-}$*Ifp35*$^{-/-}$ mice were immunized with total 200 μg of MOG_{35-55} emulsified with equal volume of CFA subcutaneously in the flank. Mice were also injected intraperitoneally 200 ng of pertussis toxin in 200 μL saline on the day of priming and 2 d later. Clinical scores of EAE mice was recorded daily according to the following 0 to 5 scale criteria as described (57): 0, no clinical symptoms; 1, mouse tail paralysis; 2, one hind limb paralyzed or both hind limbs weak; 3, mice were paralyzed in both hind limbs; 4, paralysis of both hind limbs and involvement of the forelimbs; and 5, moribund.

Lysolecithin (LPC)–Induced Cerebellar Slice Demyelination Model. The LPC-induced cerebellar slice demyelination model was based on standard protocols previously described (58). Briefly, parasagittal slices of postnatal day-3 mouse cerebellum were cut at 400 μm. The cerebellar slice was cultured in 6-well plate at the interface between air and a culture medium with culture inserts and maintained in CO_2 incubator at 37 °C for 2 wk. Then 0.5 mg · mL^{-1} LPC was added to the cultured medium and cultured for 48 h. The expression of MBP in the cerebellar slice was detected by immunofluorescent staining.

Recombinant NMI and IFP35 Protein. Full-length mNMI and the N-terminally truncated form of hIFP35ΔN protein were expressed in *Escherichia coli* strain BL21(DE3). The mNMI or hIFP35ΔN proteins was purified by nickel-nitrotriacetic acid and glutathione affinity column, respectively, and gel filtration with a Superdex 200 column (GE Healthcare) on a fast protein liquid chromatography protein purification system. Endotoxin was removed by purification with PMB chromatography.

Western Blotting. Microglia and macrophage cells were collected in radioimmunoprecipitation assay lysis buffer. The proteins were separated by sodium dodecyl sulfate-polyacrylamide gel electrophoresis (SDS-PAGE) and transferred to nitrocellulose membrane for detection with specific antibodies against iNOS, COX-2, and β-actin. For NF-κB translocation detection, cytosolic and nuclear proteins were separated as previously described (22). NF-κB (p50 and p65), IkBα, p-IkBα, and LaminB1 were detected.

Histological and Immunohistochemical Evaluation. To determine the localization of NMI and IFP35 in the CNS cells, spinal cord tissues and SH-SY5Y, C8-D1A, and BV2 cells were stained with NMI or IFP35 antibody. Antibodies for murine astrocytes (GFAP), neuron cells (NeuN), or microglia cells (CD11b) were used as a specific marker. Biotinylated goat anti-rabbit antibody and anti-mouse antibody were costained as the secondary antibody. H&E was stained for the evaluation of pathological changes, and LFB was stained for demyelination detection.

T Cell Stimulation In Vitro. Coculture of stimulated BMDCs with $CD4^+$ T Cells was performed as previously described (59). Briefly, BMDCs were isolated from bone marrow of mice and cultured with 20 ng · mL^{-1} GM-CSF and 5 ng · mL^{-1} IL4 for 5 d. The recombinant NMI or IFP35 proteins were then incubated with BMDCs for 48 h. Purified $CD4^+$ T cells were cocultured with stimulated BMDCs at the ratio of 5:1 for 5 d. The culture supernatants were analyzed for IFN-γ and IL-17A production by ELISA, and the expression of intracellular IFN-γ and IL-17A of $CD4^+$ T cells was analyzed by flow cytometry.

RT-PCR. Total mRNA was extracted from microglia and macrophages after treated with IFN-γ or IL-2. The first strand of complementary DNA was synthesized, and RT-PCR analyses were performed. The primer sequences are as follows: GAPDH: sense, 5′-CAGAACATCATCCCTGCATC-3′; antisense,5′-TACTTGGCAGGTTTCTCCAG-3′; NMI: sense, 5′-TGAGGAGCAGACAAGGGAC-3′; antisense, 5′-CAGCAACGCTAT-GGCACT-3′; and IFP35: sense, 5′-GATCCC ATTCTCAGTACCTG-3′; antisense, 5′-ACCACTAACGAGCACCCT-3′.

Flow Cytometry. For staining of B cells, we incubated cells with FITC-anti-CD3e and APC-anti-CD19b. For T cells, FITC-anti-CD3e, PerCP/Cy5.5-anti-CD8a, and PE-anti-CD4 were used. For macrophages, cells were stained with FITC-anti-CD11b and PE-anti-F4/80. For DCs, cells were incubated with FITC-anti-CD11c, PE-anti-CD80 and APC-anti-CD86. For natural killer cells, APC-anti-CD49b was used. For intracellular cytokine staining, cells were restimulated with PMA/Ionomycin and GolgiStop for 4 h, then fixed and permeabilized with Fixation and Permeabilization solution. APC-anti-IFN-γ and FITC-anti-IL-17A were used for intracellular staining. All flow cytometry was performed on a CytoFLEX flow cytometry, and data were analyzed by FlowJo version10.0.7 software.

Passive EAE Experiment and IFP35 Neutralizing Antibody Treatment. The passive EAE model was established as previously described (34). Briefly, $CD4^+$ T cells were isolated from SPs and LNs of WT and $Nmi^{-/-}Ifp35^{-/-}$ mice 12 d after EAE immunization. T cells were then cultured with $MOG_{35–55}$ (25 μg · mL^{-1}) for 4 d and adoptively transferred by intravenous injection (2×10^7 cells) to sublethally irradiated (5 Gy) WT or $Nmi^{-/-}$ $Ifp35^{-/-}$ recipient mice.

IFP35-Ab was prepared in the laboratory according to classical monoclonal hybridoma technique (49). The antibody was produced from ascites fluid of mice injected with hybridoma cells. Each mouse was intravenously injected with 100 μg (5 mg · kg^{-1}) IFP35-Ab or IgG in 100 μL sterile phosphate balanced solution. The antibody was given daily from the initial stage (day 12) to peak stage (day 22) post-immunization.

Cytokines and NO Measurement. Cytokines and NO production were measured by ELISA or Griess Reagent System according to manufacturer's instructions.

Public Transcriptomic Data Analysis. The normalized public transcriptomic dataset of gray matter tissues from MS patients and healthy control was downloaded from Gene Expression Omnibus (accession code GSE135511). The heatmap was performed by R package pheatmap. The correlation between the expression level of CD4 and IFP35 and NMI was performed by ggplot. GSEA was performed using the GSEA software (version 4.1) (60) and the data Molecular Signature Database (version 7.2) (61) using the GSEA preranked function. All analyses were performed using R version 3.6.2 (https://cran.r-project.org/).

Statistical Analysis. Experimental data are presented as mean ± SD (SD) of the mean. Cytokine production and flow-cytometric quantification results between groups were analyzed by two-tailed unpaired Student's *t* test or one-way ANOVA. Disease courses in mice were compared by two-way ANOVA followed by Tukey's post hoc tests. The linear relation signature between the expression level of CD4 and IFP35 and NMI was performed by Pearson test. *P* values of < 0.05 were considered statistically significant.

Data Availability. All study data are included in the article and/or *SI Appendix*.

ACKNOWLEDGMENTS. We thank Dr. Jin-hui Gu, Prof. Wen-bin Deng, Prof. Yu Zhang, Prof. De-yin Guo, Prof. Yuan-Chen, and Prof. Ying Jiang for valuable advice, Dr. Torsten Juelich for linguistic assistance, Prof. Liguo Zhang's laboratory for preparation of the neutralizing antibody, and Prof. Wei Tian's laboratory for preparation of the gene knock-out mice. This work was supported by the National Natural Science Foundation of China (Grants 31530015, 31870739, and 82071346), "Pearl River Talent Plan" Innovation and Entrepreneurship Team Project of Guangdong Province (Grant 2019ZT08Y464), Natural Science Foundation of Guangdong Province, China (Grant 2020B1515020035), and a Guangdong-specific project for the control of novel coronavirus (Grant 2020A111128023).

1. H. Lassmann, Multiple sclerosis pathology. *Cold Spring Harb. Perspect. Med.* **8**, a028936 (2018).
2. E. Stenager, A global perspective on the burden of multiple sclerosis. *Lancet Neurol.* **18**, 227–228 (2019).
3. B. Hemmer, M. Kerschensteiner, T. Korn, Role of the innate and adaptive immune responses in the course of multiple sclerosis. *Lancet Neurol.* **14**, 406–419 (2015).
4. N. Chihara, Dysregulated T cells in multiple sclerosis. *Clin. Exp. Neuroimmunol.* **9** (S1), 20–29 (2018).
5. Y. Dong, V. W. Yong, When encephalitogenic T cells collaborate with microglia in multiple sclerosis. *Nat. Rev. Neurol.* **15**, 704–717 (2019).
6. M. Sospedra, R. Martin, Immunology of multiple sclerosis. *Semin. Neurol.* **36**, 115–127 (2016).
7. H. Takeuchi, Neurotoxicity by microglia: Mechanisms and potential therapeutic strategy. *Clin. Exp. Neuroimmunol.* **1**, 12–21 (2010).
8. C. Larochelle, J. I. Alvarez, A. Prat, How do immune cells overcome the blood-brain barrier in multiple sclerosis? *FEBS Lett.* **585**, 3770–3780 (2011).
9. H. Tumani *et al.*, Patterns of TH1/TH2 cytokines predict clinical response in multiple sclerosis patients treated with glatiramer acetate. *Eur. Neurol.* **65**, 164–169 (2011).
10. A. Jamshidian, V. Shaygannejad, A. Pourazar, S. H. Zarkesh-Esfahani, M. Gharagozloo, Biased Treg/Th17 balance away from regulatory toward inflammatory phenotype in relapsed multiple sclerosis and its correlation with severity of symptoms. *J. Neuroimmunol.* **262**, 106–112 (2013).
11. C. S. Constantinescu, N. Farooqi, K. O'Brien, B. Gran, Experimental autoimmune encephalomyelitis (EAE) as a model for multiple sclerosis (MS). *Br. J. Pharmacol.* **164**, 1079–1106 (2011).
12. B. C. Kieseier, The mechanism of action of interferon-β in relapsing multiple sclerosis. *CNS Drugs* **25**, 491–502 (2011).
13. S.-Y. Seong, P. Matzinger, Hydrophobicity: An ancient damage-associated molecular pattern that initiates innate immune responses. *Nat. Rev. Immunol.* **4**, 469–478 (2004).
14. T. Gong, L. Liu, W. Jiang, R. Zhou, DAMP-sensing receptors in sterile inflammation and inflammatory diseases. *Nat. Rev. Immunol.* **20**, 95–112 (2020).

15. S. D. Pouwels *et al*., DAMPs activating innate and adaptive immune responses in COPD. *Mucosal Immunol.* **7**, 215–226 (2014).
16. E. Bajwa, C. B. Pointer, A. Klegeris, The role of mitochondrial damage-associated molecular patterns in chronic neuroinflammation. *Mediators Inflamm.* **2019**, 4050796 (2019).
17. A. Andersson *et al*., Pivotal advance: HMGB1 expression in active lesions of human and experimental multiple sclerosis. *J. Leukoc. Biol.* **84**, 1248–1255 (2008).
18. A. Barateiro *et al*., S100B as a potential biomarker and therapeutic target in multiple sclerosis. *Mol. Neurobiol.* **53**, 3976–3991 (2016).
19. M. Zhu, S. John, M. Berg, W. J. Leonard, Functional association of Nmi with Stat5 and Stat1 in IL-2- and IFNgamma-mediated signaling. *Cell* **96**, 121–130 (1999).
20. A. Das, P. X. Dinh, A. K. Pattnaik, Trim21 regulates Nmi-IFI35 complex-mediated inhibition of innate antiviral response. *Virology* **485**, 383–392 (2015).
21. A. Das, P. X. Dinh, D. Panda, A. K. Pattnaik, Interferon-inducible protein IFI35 negatively regulates RIG-I antiviral signaling and supports vesicular stomatitis virus replication. *J. Virol.* **88**, 3103–3113 (2014).
22. Z. Xiahou *et al*., NMI and IFP35 serve as proinflammatory DAMPs during cellular infection and injury. *Nat. Commun.* **8**, 950 (2017).
23. L. Xiong *et al*., N-myc and STAT interactor correlates with severity and prognosis in acute-on-chronic liver failure of hepatitis B virus. *J. Gastroenterol. Hepatol.* **34**, 1800–1808 (2019).
24. M. Obeidat *et al*., The effect of statins on blood gene expression in COPD. *PLoS One* **10**, e0140022 (2015).
25. L. Zhang *et al*., The role of IFI35 in lupus nephritis and related mechanisms. *Mod. Rheumatol.* **27**, 1010–1018 (2017).
26. R. De Masi, S. Orlando, IFI35 as a biomolecular marker of neuroinflammation and treatment response in multiple sclerosis. *Life Sci.* **259**, 118233 (2020).
27. J. R. Plemel *et al*., Mechanisms of lysophosphatidylcholine-induced demyelination: A primary lipid disrupting myelinopathy. *Glia* **66**, 327–347 (2018).
28. S. M. Leibowitz, J. Yan, NF-κB pathways in the pathogenesis of multiple sclerosis and the therapeutic implications. *Front. Mol. Neurosci.* **9**, 84 (2016).
29. S. M. Lunin *et al*., Immune response in the relapsing-remitting experimental autoimmune encephalomyelitis in mice: The role of the NF-κB signaling pathway. *Cell. Immunol.* **336**, 20–27 (2019).
30. M. V. Mel'nikov, M. V. Pashchenkov, A. N. Boiko, Dendritic cells in multiple sclerosis. *Neurosci. Behav. Physiol.* **48**, 668–675 (2018).
31. A. Yokota *et al*., GM-CSF and IL-4 synergistically trigger dendritic cells to acquire retinoic acid-producing capacity. *Int. Immunol.* **21**, 361–377 (2009).
32. M. Feili-Hariri, D. H. Falkner, P. A. Morel, Polarization of naive T cells into Th1 or Th2 by distinct cytokine-driven murine dendritic cell populations: Implications for immunotherapy. *J. Leukoc. Biol.* **78**, 656–664 (2005).
33. G. Wei *et al*., Global mapping of H3K4me3 and H3K27me3 reveals specificity and plasticity in lineage fate determination of differentiating CD4+ T cells. *Immunity* **30**, 155–167 (2009).
34. I. M. Stromnes, J. M. Goverman, Passive induction of experimental allergic encephalomyelitis. *Nat. Protoc.* **1**, 1952–1960 (2006).
35. E. Takemasa, S. Liu, H. Hasegawa, Production of neutralizing antibody. *Methods Mol. Biol.* **1868**, 79–92 (2018).
36. P. Scaffidi, T. Misteli, M. E. Bianchi, Release of chromatin protein HMGB1 by necrotic cells triggers inflammation. *Nature* **418**, 191–195 (2002).
37. W. Li *et al*., LPS induces active HMGB1 release from hepatocytes into exosomes through the coordinated activities of TLR4 and caspase-11/GSDMD signaling. *Front. Immunol.* **11**, 229 (2020).
38. M. Prinz, J. Priller, The role of peripheral immune cells in the CNS in steady state and disease. *Nat. Neurosci.* **20**, 136–144 (2017).
39. B. Macchi *et al*., Role of inflammation and apoptosis in multiple sclerosis: Comparative analysis between the periphery and the central nervous system. *J. Neuroimmunol.* **287**, 80–87 (2015).
40. B. A. McKenzie, V. M. Dixit, C. Power, Fiery cell death: Pyroptosis in the central nervous system. *Trends Neurosci.* **43**, 55–73 (2020).
41. D. Ofengeim *et al*., Activation of necroptosis in multiple sclerosis. *Cell Rep.* **10**, 1836–1849 (2015).
42. C. L. Hu *et al*., Reduced expression of the ferroptosis inhibitor glutathione peroxidase-4 in multiple sclerosis and experimental autoimmune encephalomyelitis. *J. Neurochem.* **148**, 426–439 (2019).
43. Z. Sternberg *et al*., High-mobility group box 1 in multiple sclerosis. *Immunol. Res.* **64**, 385–391 (2016).
44. A. Altintas, S. Akkas-Yazici, H. Tumani, V. Lehmensiek, Evaluation of CSF and serum Fetuin-A, CSF S100B and GFAP as predictive markers in multiple sclerosis (P5.211). *Neurology* **84** (14 Supplement):P5.211 (2015).
45. L. A. Peferoen *et al*., Small heat shock proteins are induced during multiple sclerosis lesion development in white but not grey matter. *Acta Neuropathol. Commun.* **3**, 87 (2015).
46. G. P. Christophi *et al*., Interleukin-33 upregulation in peripheral leukocytes and CNS of multiple sclerosis patients. *Clin. Immunol.* **142**, 308–319 (2012).
47. J. S. Roh, D. H. Sohn, Damage-associated molecular patterns in inflammatory diseases. *Immune Netw.* **18**, e27 (2018).
48. D. Bertheloot, E. Latz, HMGB1, IL-1α, IL-33 and S100 proteins: Dual-function alarmins. *Cell. Mol. Immunol.* **14**, 43–64 (2017).
49. R. Li *et al*., HMGB1 regulates T helper 2 and T helper17 cell differentiation both directly and indirectly in asthmatic mice. *Mol. Immunol.* **97**, 45–55 (2018).
50. W. Yang *et al*., Interferon-γ upregulates expression of IFP35 gene in HeLa cells via interferon regulatory factor-1. *PLoS One* **7**, e50932 (2012).
51. S. J. Lebrun, R. L. Shpall, L. Naumovski, Interferon-induced upregulation and cytoplasmic localization of Myc-interacting protein Nmi. *J. Interferon Cytokine Res.* **18**, 767–771 (1998).
52. Y. N. Paudel, E. Angelopoulou, K. C. Bhuvan, C. Piperi, I. Othman, High mobility group box 1 (HMGB1) protein in multiple sclerosis (MS): Mechanisms and therapeutic potential. *Life Sci.* **238**, 116924 (2019).
53. A. P. Robinson, M. W. Caldis, C. T. Harp, G. E. Goings, S. D. Miller, High-mobility group box 1 protein (HMGB1) neutralization ameliorates experimental autoimmune encephalomyelitis. *J. Autoimmun.* **43**, 32–43 (2013).
54. C. Barros *et al*., Inhibition of S100B prevents ex vivo demyelination and improves EAE clinical score. *Free Radic. Biol. Med.* **120**, S153 (2018).
55. J. E. Smith-Garvin, G. A. Koretzky, M. S. Jordan, T cell activation. *Annu. Rev. Immunol.* **27**, 591–619 (2009).
56. E. M. Creagh, L. A. J. O'Neill, TLRs, NLRs and RLRs: A trinity of pathogen sensors that co-operate in innate immunity. *Trends Immunol.* **27**, 352–357 (2006).
57. I. M. Stromnes, J. M. Goverman, Active induction of experimental allergic encephalomyelitis. *Nat. Protoc.* **1**, 1810–1819 (2006).
58. F. Doussau *et al*., Organotypic cultures of cerebellar slices as a model to investigate demyelinating disorders. *Expert Opin. Drug Discov.* **12**, 1011–1022 (2017).
59. F. Zhang *et al*., Anti-HMGB1 neutralizing antibody ameliorates neutrophilic airway inflammation by suppressing dendritic cell-mediated Th17 polarization. *Mediators Inflamm.* **2014**, 257930 (2014).
60. A. Subramanian *et al*., Gene set enrichment analysis: A knowledge-based approach for interpreting genome-wide expression profiles. *Proc. Natl. Acad. Sci. U.S.A.* **102**, 15545–15550 (2005).
61. A. Liberzon *et al*., The molecular signatures database (MSigDB) hallmark gene set collection. *Cell Syst.* **1**, 417–425 (2015).